ELSEVIER

Journal of Nuclear Materials 303 (2002) 99–104

journal of nuclear materials

www.elsevier.com/locate/jnucmat

Monte Carlo simulation of gas desorption process induced by low-energy ions

YiPing Chen *

Institute of Plasma Physics, Chinese Academy of Sciences, P.O. Box 1126, Hefei, Anhui 230031, People's Republic of China

Received 29 June 2000; accepted 3 April 2002

Abstract

The present paper discusses a simulated desorption phenomenon of gas chemisorbed on the surface of a solid target, induced by low-energy ions. The TRIM code is modified by introducing a cover layer of gas atoms chemisorbed on the surface of the solid target in order to simulate the desorption phenomenon. The physics model on the desorption process for the simulation is based on the Winters and Sigmund collision theory. The simulation results show that the desorption yield of gas atoms Y is linear with gas atom coverage density θ on the surface of a solid target, which is consistent with experimental results. According to the linear relation, the ion-induced desorption cross-section σ can be obtained easily. For ${}_1^1H^+ \rightarrow O/Ti$, ${}_1^2H^+ \rightarrow O/Ti$ and ${}_1^3H^+ \rightarrow O/Ti$ which usually occur in the interaction between plasma and the first wall in a controlled nuclear fusion device, σ values obtained from the simulation results are 1.57×10^{-21}, 3.64×10^{-21} and 5.38×10^{-21} m^2, respectively, for incident energy of 60 eV and at normal incidence. © 2002 Published by Elsevier Science B.V.

PACS: 52.40.-w; 52.40.Hf

1. Introduction

The Monte Carlo code TRIM is widely used for the simulation of ion–solid interactions [1,2]. By TRIM simulation of cascade movement of incident ions and atoms of a solid target in the inner solid target, the reflection coefficient of incident ions, the sputtering yield of the solid target, the depth profile of incident ions in the solid target can be obtained. In this paper TRIM is modified by introducing a cover layer of gas atoms chemisorbed on the surface of a solid target in order to simulate the desorption phenomenon of the gas atoms induced by incident ions, on the basis of the Winters and Sigmund collision theory on the desorption process [3].

Desorption phenomenon induced by incident ions occurs when the ions with sufficient energy strike the surface on which gas atoms are adsorbed. The gas desorption which is induced by incident ions is called ion induction desorption (IID). When moving ions exist in a room with high-vacuum, they strike the room wall and induce adsorbed gas to be desorbed, which causes gas pressure in the room to be raised, i.e., the degree of vacuum there is lowered. IID is a key factor which can lower the degree of high-vacuum.

In the experiments of tokamak plasma physics, the impurity gas pressure in the plasma volume must be kept at a very low level so as to reduce energy loss through impurity radiation. In fact, there are many impurity sources in tokamak plasma experiments, with one of the main impurity sources being desorption gas induced by ions coming from the core plasma.

Knowledge on the amount of desorption gas released from the first wall is very important, for example, for the control of impurities in the plasma and the design of a tokamak first-wall. IID cross-section σ is a key parameter that describes the desorption probability of IID, and it is an important parameter to calculate the desorption gas amount. Many authors have measured

* Tel.: +86-551 559 1397; fax: +86-551 559 1310.
E-mail address: ypchen@mail.ipp.ac.cn (Y.P. Chen).

0022-3115/02/$ - see front matter © 2002 Published by Elsevier Science B.V.
PII: S0022-3115(02)00854-1

σ values for some ion/target combinations [4–6] and some data have been gathered [7], but these data are for higher incident energy (>1 keV). However, in some circumstances the incident energy of ions is low. For example, the temperature of edge plasma is lower in a tokamak. So, the incident energy of ions striking the tokamak first-wall is lower (<500 eV). Experimentally, it is difficult to measure σ induced by low-energy ions, because such ions produce a very small amount of the desorbed gas atoms. So, experimental data on σ are limited to incident ions with higher energy. The present paper will discuss the simulation of the IID process using a Monte Carlo method by which we can obtain σ data easily.

Metal Ti has a high melting point. So, it can withstand high heat flux from a core plasma and is usually used as a coating layer of the first wall of a fusion experimental device or a fusion reactor. On the other hand, a Ti film has a strong function of adsorbing gas and is also usually used as an adsorption agent to pump the impurity gas in the plasma volume of a fusion experimental device or a fusion reactor in order to reduce the amount of the impurity gas. Oxygen is usually the main impurity in the fusion plasma volume and is easily chemisorbed on the Ti film. So, the present paper takes up simulation on σ for oxygen atoms chemisorbed on a Ti surface struck by ${}_1^1H^+$, ${}_1^2H^+$ and ${}_1^3H^+$ ions, respectively.

2. Simulation process

A cover layer of gas atoms chemisorbed on the surface of a target solid is introduced by modifying TRIM. According to the Winters and Sigmund collision theory on the desorption process [3], gas atoms chemisorbed on a solid surface are desorbed by ion induction through the collisions between incident ions and adsorbed gas atoms. Contributions to the desorption may come from the following three factors [3].

(1) Adsorption gas atoms are struck directly by incident ions and are reflected directly from the surface of an adsorbent solid or are reflected from inside the solid after entering it. The atoms are desorbed if their energy is greater than the desorption energy.
(2) Adsorption gas atoms collide with reflected incident ions and are desorbed if the energy is greater than the desorption energy. On the other hand, recoiled atoms may also contribute to the desorption by kicking off, on their way out, the other adsorbed atoms located on the surface of the adsorption layer.
(3) Incident ions can kick off adsorbent solid atoms, and the recoiled atoms strike adsorbed gas atoms on their way out, thus causing the desorption of adsorbed atoms.

Considering incident ions with lower energy, we may make some approximations to the Winters and Sigmund collision theory. If adsorption gas atoms are struck by incident ions, they are reflected directly from the adsorbent solid surface without entering into the interior of the solid because of the lower energy. For incident ions (especially incident light ions) with lower energy, sputtering yield of the adsorbent solid is known to be small because the energy transfer from incident light ions to heavy adsorbent atoms is small. Therefore, the contribution of sputtered adsorbent atoms to the whole desorption is considered to be negligible.

In order to illustrate above approximation to be reasonable, sputtering yield Yn is calculated for lower-energy H^+ ions vertically incident on Ti target by using Yamamura and Tawara's empirical formula which can be applied to any ion-target combination [8]. Yn is 1.90×10^{-4} (atoms/ion) for incident energy $E_0 = 100$ eV and 3.75×10^{-3} (atoms/ion) for $E_0 = 500$ eV. So, the contribution of sputtered adsorbent atoms to the whole desorption is negligible.

Using above model, our Monte Carlo simulation is performed.

3. Physics and mathematics model

A monatomic cover layer of gas atoms chemisorbed on the surface of a solid target is introduced into the simulation. Adsorbed gas exists in an atomic state in chemisorption on the target surface. If the surface coverage density of adsorbed atoms is S, the total scattering cross-section of an adsorbed atom for an incident ion σ_0 is given by

$$\sigma_0 = 1/S. \tag{1}$$

Let us assume that N_1 is the number of atoms adsorbed on the adsorbent solid surface bombarded by incident ions. When the incident ions are sampled in Monte Carlo simulation, an even distribution of the incident ions is supposed on σ_0, and the collision parameter of an incident ion P_1 can be sampled according to this distribution.

On a σ_0 surface, the distribution probability of collision parameter A_i is

$$A_i = \pi P_1^2/(N_1\sigma_0), \quad (i = 1, 2, 3, \ldots, N_1). \tag{2}$$

On the total surface $N_1\sigma_0$ bombarded by the incident ions, the probability A of the collision parameter P_1 for an incident ion is deduced as follows:

$$A = A_1 + A_2 + A_3 + \cdots + A_{N_1}. \tag{3}$$

Since, from Eq. (2),

$$A_1 = A_2 = A_3 = \cdots = A_{N_1} = \pi P_1^2/(N_1\sigma_0). \tag{4}$$

From Eq. (4), Eq. (3) becomes

$$A = \underbrace{\frac{\pi P_1^2}{N_1\sigma_0} + \frac{\pi P_1^2}{N_1\sigma_0} + \cdots + \frac{\pi P_1^2}{N_1\sigma_0}}_{N_1 \text{ terms}} = \frac{\pi P_1^2}{\sigma_0}. \tag{5}$$

So, the distribution function of the collision parameter P_1 for an incident ion $f(P_1)$ is as follows:

$$f(P_1) = \pi P_1^2/\sigma_0, \quad 0 \leqslant P_1 \leqslant \sqrt{\sigma_0/\pi}. \tag{6}$$

The inverse function $f^{-1}(x)$ of the distribution function $f(x)$ is

$$f^{-1}(x) = (\sigma_0 x/\pi)^{1/2}. \tag{7}$$

Using a direct-sampling method [9], the collision parameter P_1 can be sampled as follows:

$$P_1 = f^{-1}(R_1) = (R_1\sigma_0/\pi)^{1/2} = [R_1/(S\pi)]^{1/2}, \tag{8}$$

where R_1 is a random number uniformly distributed between 0 and 1.

When an incident ion enters the solid target interior, a series of cascade movement, which is described by TRIM [10], occurs. While being in motion, the incident ion is slowed down because of electronic and nuclear stopping of the target atoms in the material. When the energy of the incident ion is reduced to some cut-off energy, the incident ion is buried in the material. When the incident ion escapes from the solid surface during its travel, it is regarded as a reflected ion. The path of the ion movement in the material is replaced by a number of broken lines, a length of which can be obtained by sampling the distribution of atoms in the material using a model of an amorphous material. During nuclear scattering, if the energy acquired by a target atom in the material is greater than the displacement energy, the target atom can also move inside the material.

The dynamical parameters of an incident ion or a target atom in the inner target are shown as follows [10,11].

In the following equations, let us assume that N is the density of atoms in the solid target and that R_2, R_3, and R_4 are all independent random numbers uniformly distributed between 0 and 1.

An ion free-flight path in an amorphous target l is

$$l = -N^{-1/3} \ln R_2. \tag{9}$$

A collision parameter P is

$$P = \pi^{-1/2} N^{-1/3} R_3^{1/2}. \tag{10}$$

An azimuthal scattering angle θ_i is

$$\theta_i = 2\pi R_4. \tag{11}$$

Energy transfer in nuclear scattering T is defined as

$$T = \frac{4M_1M_2}{(M_1+M_2)^2} E_0 \sin^2\left(\frac{\theta_c}{2}\right), \tag{12}$$

where M_1 and M_2 are the masses of the elements involved, E_0 the incident kinetic energy, and θ_c the scattering angle in the center-of-mass system.

A flight path-length reduction due to scattering τ is

$$\tau = P \tan\left(\frac{\theta_c}{2}\right). \tag{13}$$

θ_c is derived from

$$\theta_c = \pi - 2P \int_{r_{\min}}^{\infty} \frac{dr/r^2}{\left(1 - \frac{V(r)}{E} - \frac{P^2}{r^2}\right)^{1/2}}, \tag{14}$$

where r is the interatomic separation; $r_{\min}$ is the distance of closest approach during the scattering event; $V(r)$ is the interatomic potential; P is the impact parameter; E is the relative kinetic energy. E is related to E_0 by

$$E = E_0 \Big/ \left(1 + \frac{M_1}{M_2}\right). \tag{15}$$

$r_{\min}$ is deduced from

$$1 - \frac{V}{E} - \frac{P^2}{r^2} = 0. \tag{16}$$

$V(r)$ is expressed by

$$V(r) = \frac{Z_1 Z_2 e^2}{r} \varphi\left(\frac{r}{a_1}\right), \tag{17}$$

where e is the electronic charge, Z_1, Z_2 the atomic numbers of the elements involved, a_1 the screening length, and $\varphi(r/a_1)$ the screening function. We have employed the Molière potential approximation to the Thomas–Fermi potential. Thus,

$$\varphi\left(\frac{r}{a_1}\right) = 0.35e^{-0.3r/a_1} + 0.55e^{-1.2r/a_1} + 0.1e^{-6r/a_1}, \tag{18}$$

$$a_1 = \mathrm{CA}\, a, \quad a = \frac{0.8853 a_0}{(Z_1^{1/2} + Z_2^{1/2})^{2/3}}, \tag{19}$$

where a_0 is the Bohr radius, and CA is the correction factor.

Energy loss in the flight path ΔE due to electronic stopping is calculated by using a calculation formula that takes account of the Oen–Robinson energy loss model (OR) [11]. This OR model depends on the distance of closest approach in a binary collision, and its energy loss ΔE_{OR} is given by

$$\Delta E_{\mathrm{OR}} = \frac{0.045 k \sqrt{E}}{\pi a_1^2} e^{-0.3 r_{\min}/a_1}. \tag{20}$$

If ΔE_{OR} takes up 50% of energy loss ΔE, ΔE is calculated by

$$\Delta E = 0.5\Delta E_e + 0.5\Delta E_{OR}, \tag{21}$$

where ΔE_e is the continuous energy loss and is calculated by

$$\Delta E_e = N \int_0^1 S_e(E)\,dl, \tag{22}$$

where $S_e(E)$ is the electronic stopping cross-section. We have adopted the Lindhard–Scharff energy loss model [10] given by

$$S_e(E) = kE^{1/2}, \tag{23}$$

where the Lindhard electronic stopping coefficient k is expressed by

$$k = \frac{1.212 Z_1^{7/6} Z_2}{(Z_1^{2/3} + Z_2^{2/3})^{3/2} M_1^{1/2}} \ (\mathrm{eV}^{1/2}\mathrm{\AA}^2). \tag{24}$$

IID follows the following formula, as was proved indirectly by experiments [3]:

$$\theta = \theta_0 e^{-j\sigma t}, \tag{25}$$

where θ is the surface coverage density of gas atoms adsorbed on the adsorbent surface at time t, θ_0 the initial surface coverage density, j the flux density of incident ions, and σ the IID cross-section.

From above experimental formula, the following deduction can be made:

$$\frac{d\theta}{dt} = \theta_0 e^{-j\sigma t}(-j\sigma) = -j\theta\sigma.$$

Let

$$Y = -\frac{1}{j}\frac{d\theta}{dt}.$$

So,

$$Y = \sigma\theta, \tag{26}$$

where Y is the IID yield. It is clear from Eq. (26) that Y is linear with θ and that the slope of the line is equal to σ. Thus, if the linear relation is obtained from simulation, then the σ value can be obtained easily.

4. Simulation results

Figs. 1–3 show some results of the simulation. The calculated data on Y versus θ are marked with the symbols of circles and squares in these figures. Figs. 1 and 2 show Y of oxygen atoms chemisorbed on the Ti surface versus θ of oxygen atoms for $^1_1H^+$ ions incident on O/Ti target and at normal incident, i.e. $^1_1H^+ \rightarrow$ O/Ti, with incident energy E_0 of 30, 60 and 100 eV. For comparison, Fig. 3 shows Y for $^1_1H^+$, $^2_1H^+$ and $^3_1H^+$ ions incident on O/Ti target at normal incidence, i.e. $^1_1H^+ \rightarrow$ O/Ti, $^2_1H^+ \rightarrow$ O/Ti, $^3_1H^+ \rightarrow$ O/Ti, respectively, for $E_0 = 60$ eV. In these figures, YITA is the incident angle of ions to the target surface normal; N_s is the number of atoms desorbed which is set in the simulation. The good-fit straight lines to the calculated data are drawn in Figs. 1–3. It is clear from these figures that the lines are in good agreement with the data. Thus, Y is shown to be approximately linear with θ, which is consistent with the formula (26). At the same time, it can also be seen from these figures that larger dispersion of the simulation data from the linear relation exists for lower incident energy, for example, $E_0 = 30$ eV. With the increase of E_0 the dispersion decreases. For low incident

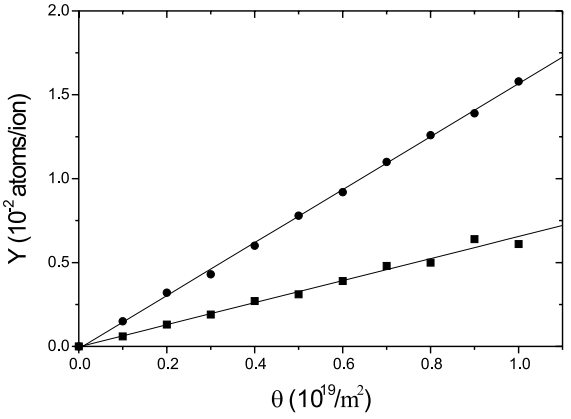

Fig. 1. Relation between yield of oxygen atoms Y and surface coverage density θ chemisorbed on Ti solid target $^1_1H^+ \rightarrow$ O/Ti, YITA = 0°, $N_s = 10\,000$, (■) $E_0 = 30$ eV, (●) $E_0 = 60$ eV.

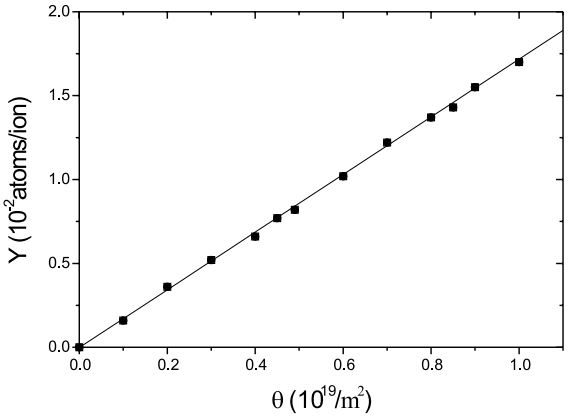

Fig. 2. Relation between yield of oxygen atoms Y and surface coverage density θ chemisorbed on Ti solid target $^1_1H^+ \rightarrow$ O/Ti, YITA = 0°, $N_s = 10\,000$, $E_0 = 100$ eV.

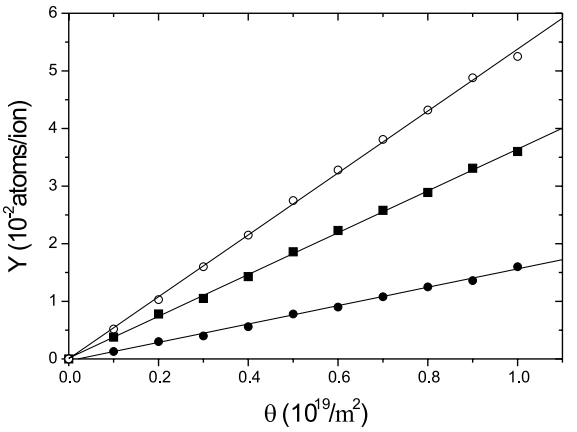

Fig. 3. Relation between yield of oxygen atoms Y and surface coverage density θ chemisorbed on Ti solid target YITA = 0°, $N_s = 10\,000$, $E_0 = 60$ eV, (•) ${}^1_1H^+ \rightarrow O/Ti$, (■) ${}^2_1H^+ \rightarrow O/Ti$, (○) ${}^3_1H^+ \rightarrow O/Ti$.

energy $E_0 \leqslant 30$ eV, the binary approximation may become deteriorated. So, the model for the simulation must be changed for low E_0, but which is very difficult within the framework of the binary approximation.

σ for ${}^1_1H^+$, ${}^2_1H^+$ and ${}^3_1H^+$ ions, respectively, are obtained by evaluating the slope of the straight lines shown in the figures. Some σ data thus obtained for YITA = 0° are tabulated in Table 1. For ${}^1_1H^+ \rightarrow O/Ti$, σ versus E_0 is shown with the symbol of closed circles in Fig. 4. The solid line in the figure guides the eye. From Fig. 4, it can be seen that σ has a peak value for E_0 of about 150 eV and $\sigma = 0$ for $E_0 = E_b = 7.66$ eV. Since oxygen is adsorbed as an atom and sputtered as an atom, a binding energy (adsorption energy) E_b for the sputtering calculation is estimated approximately to be one-half the dissociation energy E_d added to one-half the measured heat of adsorption q_c [3], i.e. $E_b = (E_d + q_c)/2$. For the oxygen atoms adsorbed on the Ti surface, $E_d = 117.1$ kcal/mol, $q_c = 236$ kcal/ mol, which yields $E_b = 7.66$ eV/atom.

As was discussed in Section 2, the contributions to σ are due to incident ions and reflected ones. For ${}^1_1H^+ \rightarrow O/Ti$, the rate of contribution of reflected ions to σ, η, versus E_0 is shown in Table 2.

Table 1
A part of simulation values of σ (m^2), (YITA = 0°)

E_0 (eV)	${}^1_1H^+ \rightarrow O/Ti$	${}^2_1H^+ \rightarrow O/Ti$	${}^3_1H^+ \rightarrow O/Ti$
30	0.66×10^{-21}		
60	1.57×10^{-21}	3.64×10^{-21}	5.38×10^{-21}
100	1.71×10^{-21}		
200	1.75×10^{-21}		
500	1.18×10^{-21}		

Fig. 5 shows the average vertical range of incident ${}^1_1H^+$ ions in the adsorbent Ti interior R in units of Å versus θ for $E_0 = 30$ eV and at normal incidence. The solid line in the figure guides the eye. The oxygen atoms adsorbed on the Ti surface may have resistive action to incident ions because of the collisions between them, which results in the decrease of R with the increase of θ. From Fig. 5 it can be seen that R is 18.05 Å for $\theta = 1 \times 10^{19}$ m^{-2}, compared to 19.50 Å for no surface coverage density.

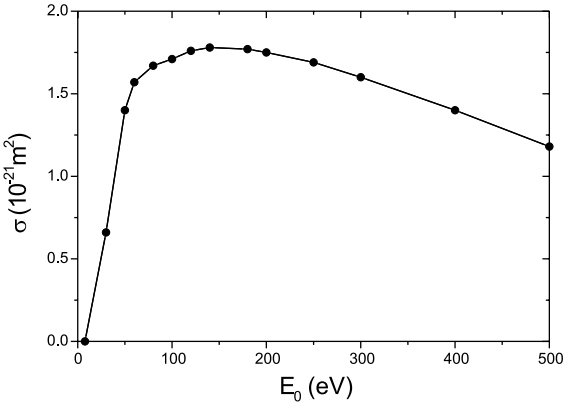

Fig. 4. Relation between desorption cross-section σ and incident energy E_0 ${}^1_1H^+ \rightarrow O/Ti$, YITA = 0°, $N_s = 10\,000$.

Table 2
Contribution rate η of reflected ions to σ, (YITA = 0°)

E_0 (eV)	30	60	100	200	500
η (%)	0	15	33	40	38

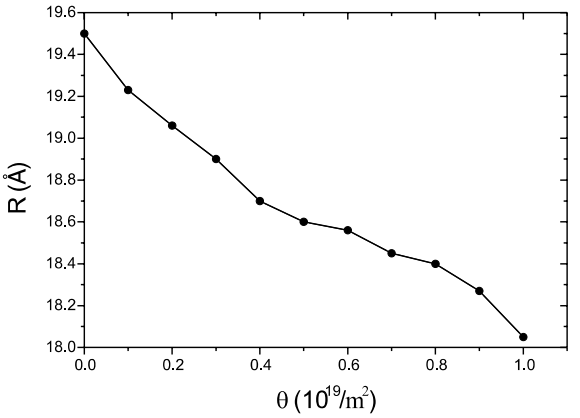

Fig. 5. Relation between average vertical range R and surface coverage density θ chemisorbed on Ti solid target ${}^1_1H^+ \rightarrow O/Ti$, YITA = 0°, $N_s = 10\,000$, $E_0 = 30$ eV.

5. Summary

Monte Carlo simulation of gas desorption process induced by energetic ions is an important method to evaluate IID cross-section σ, especially for low-energy incident ions striking a surface on which gas is adsorbed, because only very little experimental data exist for low incident energy. The simulation results obtained in this paper show that the desorption yield of gas atoms Y is linear with the coverage density θ of gas atoms on the target surface, which is consistent with the experimental results. From the linear relation, σ can be obtained easily. We have indicated that σ has a peak value for E_0 of about 150 eV for ${}^{1}_{1}H^{+} \rightarrow O/Ti$ at normal incidence; oxygen atoms adsorbed on the Ti surface may have resistive action to incident ions; some σ values for ${}^{1}_{1}H^{+} \rightarrow O/Ti$, ${}^{2}_{1}H^{+} \rightarrow O/Ti$ and ${}^{3}_{1}H^{+} \rightarrow O/Ti$ have also been obtained.

Usually atoms are adsorbed on a solid target as atomic state and they form a monatomic layer in chemisorption, as was considered in this paper. Monte Carlo simulation of gas desorption process induced by energetic ions for more complex cases, for example, for the multi-atomic layer or the multi-molecular layer adsorption, will be carried out in future. In addition, the contribution of sputtered adsorbent atoms to the whole desorption and the model modification of the interactions between very low-energy incident ions and a solid target for the simulation will also be considered.

Acknowledgements

This work was supported by the Chinese National Science Foundation (Grant no. 19785003).

References

[1] J.P. Biersack, W. Eckstein, Appl. Phys. A 34 (1984) 73.
[2] E. Taglauer, in: R.A. Langley, J. Bohdansky, W. Eckstein, P. Miodusyewski, J. Roth, E. Taglauer, E.W. Thomas, H. Verbeek, K.L. Wilson (Eds.), Nuclear Fusion Special Issue, IAEA, Vienna, 1984, p. 43.
[3] H.F. Winters, P. Sigmund, J. Appl. Phys. 45 (11) (1974) 4760.
[4] S. Sukenbu, Y. Gomay, J. Nucl. Mater. 128&129 (1984) 775.
[5] E. Taglauer, W. Heiland, J. Nucl. Mater. 93&94 (1980) 823.
[6] R. Bastaze, J. Nucl. Mater. 93&94 (1980) 830.
[7] A. Sagara, K. Kamada, J. Nucl. Mater. 111&112 (1982) 812.
[8] Y. Yamamura, K. Sakaoka, H. Tawara, NIFS-DATA-31, 1995.
[9] L.C. Fei, X.Z. Chang, Monte Carlo Method and Its Application in Particle Transformation Question, Science Publishing House, 1980 (in Chinese).
[10] J.P. Biersack, L.G. Haggmark, Nucl. Instrum. and Meth. 174 (1980) 257.
[11] W. Takeuchi, Y. Yamamura, Radiat. Eff. 71 (1983) 53.